UNIVERSITÀ DEGLI STUDI DI PADOVA

Dipartimento di Fisica e Astronomia "Galileo Galilei"

Corso di Laurea in Fisica

Tesi di Laurea

Solar Radiation Alert System on Mars:

optimal orbits for a swarm of early-warning cubesats

Relatore

Prof. Denis Bastieri

Correlatore

Prof. Riccardo Rando

Laureanda

Federica Borgato

Anno Accademico 2018/2019

Contents

Introduction

The very first Mars settlement is becoming a reality and with the approaching of this event more practical aspects of the permanence of humans on Mars start becoming relevant. Radiation is an invisible enemy, but one of the most dangerous ones once the astronauts reach the Mars soil: the interest of space agencies on long duration mission makes fundamental the need of an accurate dosimetry analysis. Other experiments already studied ionizing radiation on Mars soil, such as the experiment RAD onboard the rover Curiosity.
One of the possible threats to the astronauts' health are the high energy particles that the Sun emits during its cicle: these are called Solar Energetic Particles (SEPs) and are associated to flares and coronal mass ejections. The unpredictability of this kind of events makes necessary to have an "alarm system" for Mars human settlers, because SEPs are rare but may be deadly.
The idea is to use CubeSats, nanosatellites known for their high performances and low cost, to create a swarm around Mars in order to always have one of them between the Red Planet and the Sun: in this way it is possible to reveal a SEP event and give an alert to humans who can shield themselves properly.

The framework of this thesis is the project "White Book on Mars", that involves all the aspects of a future human settlement on Mars, starting from Pshycology, Medicine, Economy, Engeneering going to Physics and other topics. This present work provides a first analysis of dosimetry on Mars, i.e. the monitoring of ionizing radiation in order to reduce health hazards for astronauts.

The aim of the present work is to optimize the orbit of a CubeSats Swarm in order to provide an effective Solar Radiation Alert System for human Mars settlers through the use of the Gmat Nasa's simulator. In Chapter 1 are exposed all the hazards due to the ionizing radiation on Mars and its main sources. In Chapter 2 are explained the CubeSats' features and performance, while in Chapter 3 there is the optimization of orbits for the CubeSats' Swarm.

Chapter 1

Settling on Mars: Effects of Ionizing Radiation

1.1 Ionizing radiation and health-risk mitigation

The focus of space agencies on long duration space missions lead to the necessity of evaluating exposure to the hazards of severe space radiation. Fundamental to the risk mitigation is the advance in knowledge of the main charateristics of the radiation in order to provide technology to guarantee safe human missions. There have been several missions either in deep space or on planets like Mars to evaluate the amount of ionizing radiation, such as RAD.
To evaluate the dangerousness of the radiation, esperiments measure the dose. Dose is a purely physical quantity, with units of Gray or milligray (1 Gray=1 J/kg) and represents energy imparted by radiation per unit mass onto an absorbing material. Equivalent dose is the expression of dose in terms of its biological effect. When measuring radiation energy another consideration is that equal doses of all types of ionizing radiation do not produce the same harmful biological effects.

The medium equivalent dose that a human absorbs on Earth is about 3mSv thanks to the atmosphere that shields from high energy particles and the planet's magnetic field that deflects most of them. In deep space the radiation is free to interact with anything on its way so that the astronauts need to be provided with adeguate protection and, most of all, their space journey must be short in order to prevent serious health damages.

Ionizing radiation, due to its high energy, damages nucleic acids tampering with the instructions they have encoded for cell reproduction and functionality; these may lead to cancer or other desease.
Figure 1.1 shows that the equivalent dose of 500 days on Mars is about 100 times the one on Earth on a year and that's why it's so important to study the radiation in order to provide adequate shielding for further space journeys.

1.2 Ionizing radiation on Mars

The radiation exposure on Mars surface is more intense than the one on Earth due to two main factors:

- Mars lack a global magnetic field to deflect energetic charged particles.
- Martian atmosphere is much thinner ($< 1\%$) than the one on Earth and this is why there's a little shielding against the high energy particles that are incident at the top of its atmosphere.

There are two main kinds of ionizing radiations, Galactic Cosmic Rays (GCRs) and Solar Energetic Particles (SEPs). Both interact with the atmosphere and, if they have high energy, penetrate into the Martian soil where they produce secondary particles (such as neutrons or $\gamma-$rays).

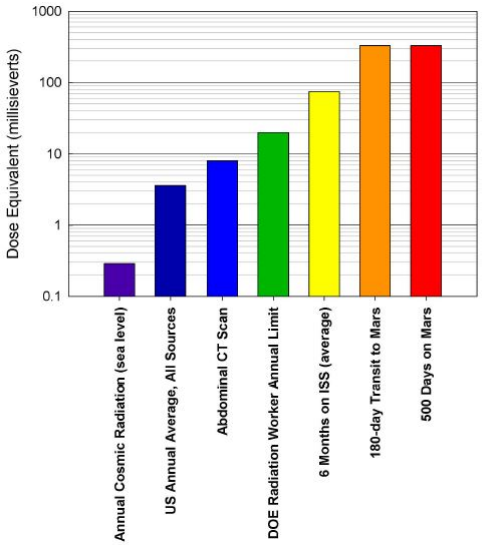

Figure 1.1: Comparison of the radiation dose equivalent for a 500 day surface stay to that from a 180 day transit to Mars, a six month stay on the International Space Station (ISS), and several earth-based sources of radiation.

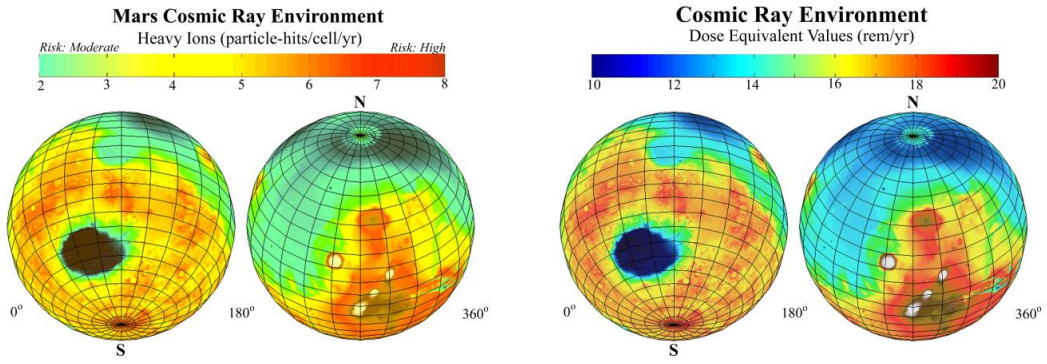

Figure 1.2: On the left, the estimated radiation dosages from cosmic rays reaching the surface. On the right, the doses of high-energy-particle cosmic radiation reaching the surface. Both data from MARIE orbital radiation data and MOLA laser altimetry (Image Credit: NASA/Jet Propulsion Laboratory/JSC).

1.2.1 Galactic Cosmic Rays (GCRs)

GCRs originate outside the solar sistem and are mostly produced in supernova remnants. These are high energy particles (10 MeV/nuc to $>$ 10 GeV/nuc), consist in nuclei fully ionized so that they interact with and are influenced by magnetic fields. GCRs are modulated by the heliosphere and anti-correlated with solar activity.

The solar cycle have an average duration of about 11 years and reflects magnetic activity; various magnetically driven solar phenomena follow the solar cycle, including sunspots and coronal mass ejections. The solar wind modulates the flux of GCRs coming to Mars so that the majority of them can't reach the planet during solar maximum. When there's a solar minimum, due to the abscence of phenomena like coronal mass ejections, GCRs have easier access to Mars. But unlike the solar cycle, the GCR spectrum remains relatively constant in energy and composition, varying only slowly with time.

GCR permeate interplanetary space and is comprised of roughly protons ($85-95\%$), helium ions ($10-13\%$), electrons (1%) and heavier ions (1%); composition varies depending on solar modulation. GCR is extremely damaging to materials and biological tissues.

Figure 1.2 represents how the radiation is distributes on Mars surface. On the left, the figure shows the estimated radiation dosages from cosmic rays reaching the surface. The colors in the map refer to the estimated annual dose equivalent in rems, a unit of radiation dose. The range is generally from 10 rems (color-coded dark blue) to 20 rems (color-coded dark red). On the right, the figure shows the estimates for the doses due to high-energy-particle cosmic radiation reaching the surface. Colors in the map refer to the estimated average number of times per year each cell nucleus in a human there would be hit by a high-energy cosmic ray particle. The range is generally from two hits (color-coded green), a moderate risk level, to eight hits (coded red), a high risk level. In both cases, the lower the altitude, the lower the expected dose, because the atmosphere provides shielding, despite a very modest one.

1.2.2 Solar Energetic Particles (SEPs)

Solar Energetic Particles are produced in the solar corona and observed in interplanetary space; they're due to high energy processes, and come in association with solar dynamic events such as flares and coronal mass ejections. SEPs are rare and difficult to predict, with duration from minutes to days and several orders of magnitude. They're mainly composed by protons, but the composition depends on the particular event. It's possible to divide SEPs events in "soft spectrum" events and "hard spectrum" events, depending on how energetic are the particles.

- "Soft spectrum" events presents proton and helium nuclei with energies below 150MeV/nuc, so that they are not able to reach Martian soil due to interactions with the atmosphere.
- "Hard spectrum" events, ions can be accelerated to energies above 150MeV/nuc and they can reach the Martian surface.

The risk of exposure to SEPs increases with solar activity. Another distinction of SEPs can be made considering their duration and other features. We can distinguish two kinds of SEPs.

- *Gradual Events*: their duration is days, there's a small electron/proton fluence ratios. The composition is variable and they're associated with both large solar flares and fast coronal mass ejections (CMEs), also with solar type II radio bursts. Gradual events are believed to be due to acceleration by CME driven shocks. They tipically happen in Solar Maximum.
- *Impulsive Events*: their duration is days, there's a large e/p ratio, dominated by low energy electrons 1 to 100 keV and ions 0.01–1 MeV/nuc. There is also an enhanced alpha/proton ratio and impulsive events are associated with solar type III radio bursts. Their frequency is more than 10^3/year.

In Figure 1.3 it is possible to see the different signals produced by the two kinds of SEP events. In the impulsive event, there are solar flare accelerated particles and no shock. In the gradual event, there are shock-accelerated particles. These features are also visible in Figure 1.4: impulsive events particles are accelereted in lower atmosphere, in gradual events particles are given acceleration by shocks in corona.

In general, acceleration may be caused by several events, such as diffusive shock acceleration, shock drift and shock surfing (as previously discussed), resonant wave-particle interactions, turbolence, magnetic reconnection, quasi-static electric fields (Figure 1.4(right)).

1.3 RAD experiment on Mars

In order to understand how radiation can practically influence human settelments, it's important to know some real data about Mars' surface radiation environment.

The Radiation Assessement Detector (RAD) on the Mars Science Laboratory's Curiosity rover made detailed measaurements of the GCRs and SEPs on the surface of Mars for about 300 Sols from 17 August 2012 to 1 June 2013.

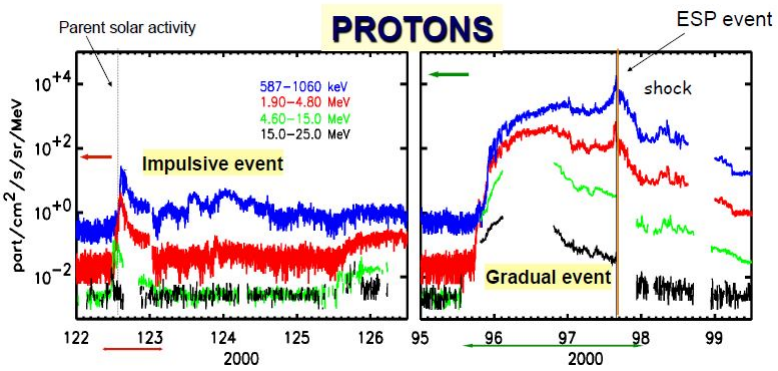

Figure 1.3: SEP time profiles measured by EPAM proton telescope (two low energy channels) onboard ACE spacecraft and by CPME detector (two high energy channels) onboard IMP-8 satellite.

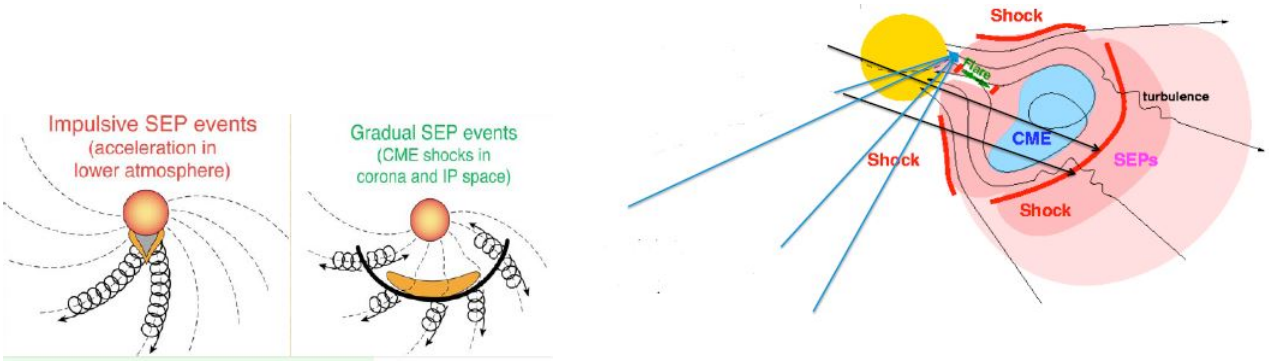

Figure 1.4: SEP different accelerations depending on the type of event(left), and main causes of the acceleration(right).

Figure 1.5 shows the trend of GCRs' dose rate in function of time. It varies by a few percent due to diurnal change in Mars' atmosphere, indeed there's an anticorrelation between dose rate and atmospheric pressure (Figure 1.6). This effect is related to the daily termal tides that Mars experiences each Sol: the direct heating of the Martian atmosphere by the Sun creates global scale waves that redistribuite atmospheric mass.

In Figure 1.5 it's possible to see a SEP event (happened on $11 - 12$ April 2013, Sol 242), the first "hard spectrum" event seen by RAD. The SEP dose was obtained by substracting the average GCR dose rate for the duration of the SEP event (Figure 1.7). Its energy spectrum was hard enough to produce an enhancement of 30% over the standard GCR dose.

Several SEP events were reported and modeled to be much more intense than the ones seen by RAD. In order to prevent health damages for future astronauts on Mars due to this kind of event, it could be important to have an alarm system in order to warn humans on Mars' surface to protect themself using harder shieldings or going in an underground base. This can be provided by CubeSat Swarms put around Mars, as we'll see on Chapter 3.

The anomalous deep minimum in Figure 1.7 is due to the shutdown of RAD in order to activate other facilities on board of Curiosity.

The results of RAD experiment are reported on Table 1.1.

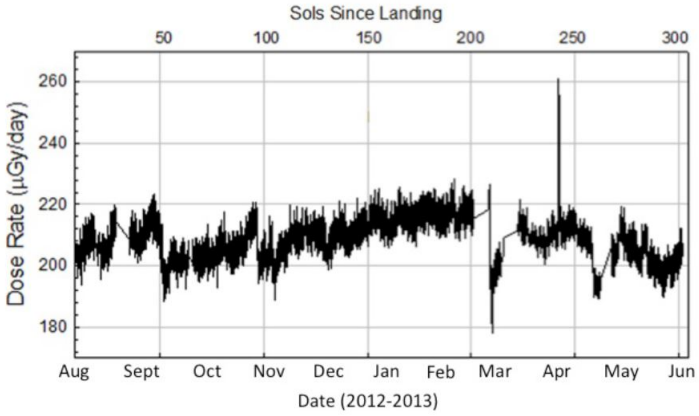

Figure 1.5: Time series of radiation dose rate of GCRs measured by RAD on Mars' surface.

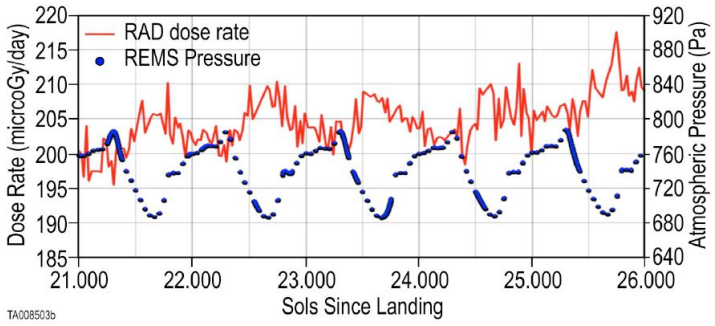

Figure 1.6: Comparison of RAD dose rate vs time and REMS atmospheric pressure.

Table 1.1: Results of RAD experiment on dose and dose equivalent of GCRs and SEPs.

GCR Dose Rate [mGy/day]	GCR Dose Equiv. Rate [mSv/day]	SEP Dose [mGy/event]	SEP Dose Equivalent [mSv/event]
0.210	0.64	0.025	0.025

Dose equivalent of GCRs on Mars is three times the one absorbed in a year on Earth, while the SEPs events give a little contribution to the whole dose (as said earlier, RAD detected a SEP event not much intense: other events could give a much greater contribution). This level of dose equivalent is really harmful for humans' health.

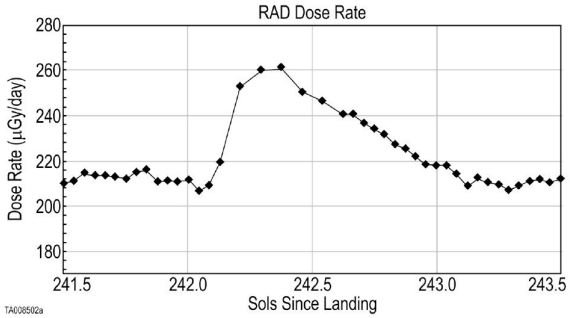

Figure 1.7: Dose rate enhancement from a solar energetic particle event observed by RAD on Sol 242, while Mars was in solar conjunction.

Chapter 2

A Dosimeter on-board a Cubesat

2.1 CubeSat features

A CubeSat is a standardized model of miniaturized satellite with precise restrictions for both volume and weight: it is based on a $10 \times 10 \times 10 \text{cm}^3$ cubic unit with a maximum weight of 1.33kg (1U CubeSat). We study a payload compatible with 1U standard. In particular we are planning to use a nano-satellite as a MeV Telescope, since the electromagnetic spectrum around 1MeV is not so thoroughly explored. The target is to study the viability of a nano-satellite Compton telescope, based on the CubeSat architecture. The satellite is assumed to be operating in a quasi-equatorial low orbit, pointing at the zenith.

- The structure is made of five CsI(Tl) calorimeters, one on the bottom and four on the sides of the CubeSat, as shown in Figure 2.1. CsI(Tl) crystals are a material that produces good performances and was already tested by previous missions. they are also very cheap compared to the tracker and do not affect significantly the cost of the detector. The readout system of the CsI crystals has been optimized by using Silicon photomultipliers. The number of channels is small compared to that of the tracker.

- The tracker is based on a Silicon-strip detector technology (SSD) and its spatial resolution is 500 μm. The tracker for a Compton Telescope needs Double-Sided Strip Detectors (DSSDs) in ordere to obtain information about electrons' direction.

- A plastic anti-coincidence surrounds the detector to shield it from charged paricles. It's composed of several layers of plastic scintillator, each 5 mm thick, read by silicon photomultipliers. In this way it is possible to reject the charged background.

- No readout electronics and support materials are yet included into the design: by adding them, it could affect significantly effective area and sensitivity.

On Table 2.1 there are some design specifications.

Table 2.1: Design specifications

Parameter	Value or Range
Si Tracker: layer area	$7.4 \times 7.4\,\text{cm}^2$
Si Tracker: layer thickness	500 μm
Si Tracker: number of layers	30
Si Tracker: strip pitch	500 μm
Calorimeter: crystal dimension	$0.5 \times 0.5 \times 7.5\,\text{cm}^3$
Calorimeter: depth resolution (1σ)	0.5 cm
ACD: thickness	0.5 cm

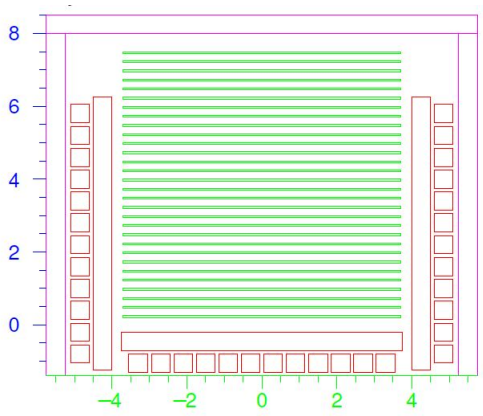

Figure 2.1: The active detectors of the MeV cubesat. In green, the Si tracker; in red the Cesium Iodine calorimeter; in magenta the anti-coincidence detector. For clarity we have removed the front and back calorimeter modules; scales in cm.

2.2 Detector Performace Parameters

In general, the performance of a telescope is characterized in terms of effective area, energy resolution and angular resolution (assumed to be independent from one another).

Angular resolution is defined by two quantities:

- Angular Resolution Measure (ARM): quantifies how precisely the direction of the scattered photon has been reconstructed. It's given by the difference of real and measured scatter angle.
- Scatter Plane Deviation (SPD): quantifies how well the electron track is reconstructed. I's given by the difference between the actual scatter plane and the mesured one.

Using both ARM and SPD, it's possible to define a final angular resolution element on the sky map.

2.3 Simulation methodology and performance estimate

The performance of this kind of CubeSat has already been estimate by simulation considering it on a Low Earth Orbit (LEO; 500km, equatorial). The main background contributions are as follows.

1. Extra-Galactic Background: a diffuse, hisotropic, homogeneous photon background.
2. Earth's Gamma Emissions: due to the interaction of primary cosmic rays and the atmosphere.
3. Charged Background: events due to charged cosmic rays hitting the detector.
4. Activation: the continuos flux of cosmic rays activates the satellite materials. This contribution scales with the amount of passive material in the telescope.

Background fluxes were measured in previous missions. Given the energy range and the planned orbit, the main contribution to the background due to charged particles is caused by secondary electron.

The estimate of the sensitivity of the detector is also suitable for a CubeSat on an orbit around Mars, since there the main contribution to the background are GCRs and its atmosphere is very little, so that the interactions are minimal.

In the simulation, data are divided into different event classes: tracked and untracked. Selecting only tracked events allows to improve the angular resolution element at expense of the effective area. The use of untracked events guarantees a greater effective area, but the angular resolution worsens.

The sources of background considered are the photons produced by the interactions of primary protons with the atmosphere and the isotropic photon background. The residual contamination by charged particles passing the ACD is negligible compared with the other sources.

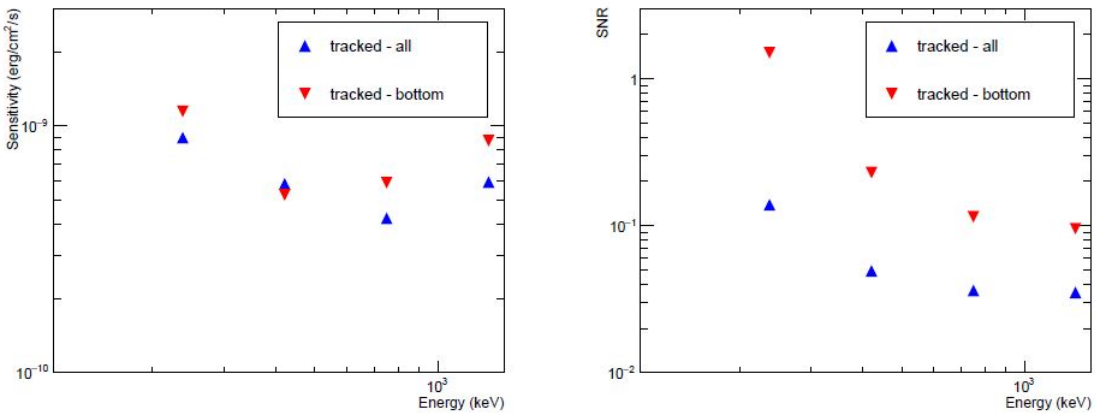

Figure 2.2: Sensitivity for a steady point source (3 sigma and $T_{eff} = 106$ s, left) and signal-to-noise ratio (same T_{eff} , at the sensitivity limit, right) as a function of energy for an inclination $\theta < 14,5$ degrees.

The software used in the simulation is Megalib toolkit (Zoglauer et al. 2008). It simulates the all the photon sources (10^5s) and then the background rate is computed counting how many events intersect the location of a candidate point source at a given inclination, considering the angular resolution as a function of energy and inclination (ARM for all events, SPD only for "tracked" events). The Megalib toolkit automatically rejects kinematically unlikely events. Despite that, some accepted events are reconstructed toward the wrong sky position due to incomplete absorption. This results in an additional quasi-isotropic background component and accounted in our simulation.

In Figure 2.2(left) is shown the 3-σ sensitivity for an observation with $T_{eff} = 10^6$s for all "tracked" events revealed only in the bottom calorimeter assembly ("tracked" bottom). In Figure 2.2(right), there's the signal-to-noise ratio for the same data set. At the lower energies, the tracked-bottom events mantain a signal-to-noise ratio greater than 10% across the full energy range of the instrument, while there's a 30% decrease in sensitivity realteive to all track events. A succesfull observation at a given S/N implies that the systematic uncertainties are kept under control at the same level. 10% is a reasonable goal.

Since now, it's been assumed that the point source was at zenith, aligned with the satellite. In Figure 2.3 is shown the point source sensitivity (same conditions) as a function of the inclination of the incoming photon (with energy in the band $562 - 1000$keV). Until 90 degrees there's no loss of field of view. Beyond that the brightness of Earth's horizon causes significant complications.

Untracked events can be discarded in the case of observation of faint, steady sources, due to the poor S/N ratio ($< 1\%$).

The nominal energy range of the detector is 100keV-5MeV, despite of that the analysis is limited to $E < 1.78$MeV because beyond that point the amount of badly reconstructed events become relevant. Such cuts depends on the exact geometry and read out of the satellite.

2.4 Purpose of a CubeSat around Mars

The advantages of nano-satellites are their great performances and low cost. The CubeSat in object in particular is equipped with a silicon microstrip detector that reveals ionizing radiation in such a way as to operate as a dosimeter. There can be different employement areas for this kind of nano-satellites, in this case we want them to work as an alert system for astronauts on Mars: in presence of SEPs, these CubeSats have to send an alarm signal to the settlers to let them protect themself by going to the underground shelter. In this way the health damages due to ionizing radiation can be minimized.

Some nano-satellites with CubeSat architecture are already in orbit around Earth (for example, to control climate changes), but only in 5 May 2018 two CubeSats, MarCo A e MarCo B, where launched on a Nasa mission to Mars to monitorate the lander Insight. They were the first of this kind of

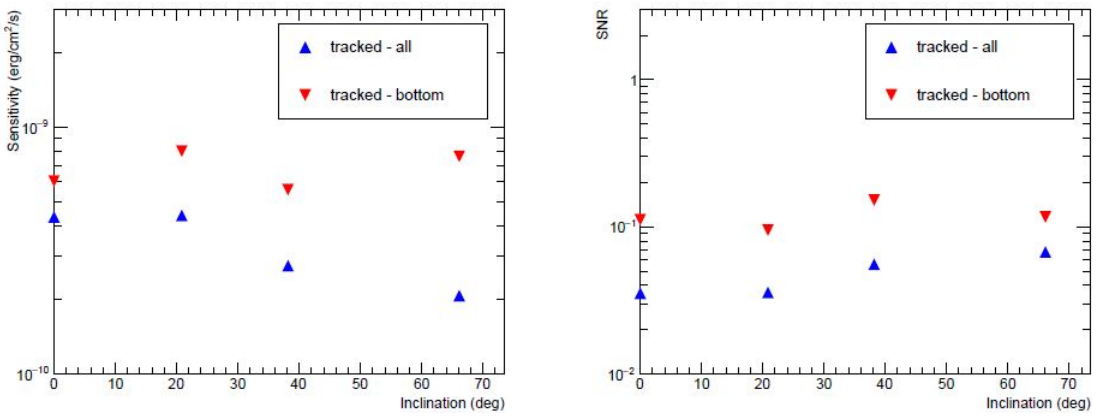

Figure 2.3: Sensitivity for a steady point source (3 sigma and $T_{eff} = 106$ s, left) and signal-to-noise ratio (same T_{eff} , at the sensitivity limit, right) as a function of inclination from the axis for 562 keV $<$ E $<$ 1 MeV.

spacecraft to fly to deep space. This mission clarified that this kind of technology can work properly and be usefull for missions on Mars.

Chapter 3

Optimization of Cubesat Swarms in Orbit around Mars

3.1 General Mission Analysis Tool (GMAT)

The software used to simulate the orbits of swarms of CubeSats around Mars is GMAT. General Mission Analysis Tool (GMAT) is an open source trajectory design and optimization system developed by NASA and private industry. It is designed to model and optimize spacecraft trajectories in flight regimes ranging from low Earth orbit to lunar applications, interplanetary trajectories, and other deep space missions. Analysts model space missions in GMAT by first creating resources such as spacecraft, propagators, and optimizers to name a few. These resources can be configured to meet the needs of specific applications and missions. After the resources are configured they are used in the mission sequence to model the motion of spacecraft and simulate events in a mission's time evolution. The system can display trajectories in space, plot parameters against one another, and save parameters to files for later processing.

3.1.1 Orbital elements

To uniquely identify a specific orbit is necessary to know some parameters called the orbital elements; there are many different ways to mathematically describe the same orbit. A real orbit changes with the passing of time because of gravitational perturbations and the effects of relativity; despite that, given an inertial frame of reference and an arbitrary epoch, it's necessary to have six orbital parameters in order to unambiguosly identify an orbit. This happens because the problem contains six degrees of freedom.
The traditional orbital elements are the six Keplerian elements. The shape and the size of the ellipse are defined by *eccentricity* (ECC) and the *semimajor axis* (SMA, sum of the periapsis and apoapsis distances divided by two). The orientation of the orbital plane is given by *inclination* (INC) and the *longitude of the ascending node* (RAAN). The remaining two elements are the *argument of periapsis* (AO) and the *true anomaly* (TA).
To define these orbital parameters is fundamental to have a plane of reference, that is usually the ecliptic plane for satellites in solar system. Depsite that, I chose as a plane of reference the Mars equatorial plane, since I studied equatorial orbits.

3.1.2 CubeSat Swarm

I studied a swarm composed by three CubeSats, equally distribuited in space in order to have always one of the CubeSats between Mars and the Sun.
I set the weight of the three CubeSats at 8 kg (about a 6U CubeSat).
To define properly the orbital parameters of the CubeSats, in the simulation I used as coordinate system the axes type MJ2000Eq centered on Mars: this is an inertial coordinate system. The nominal

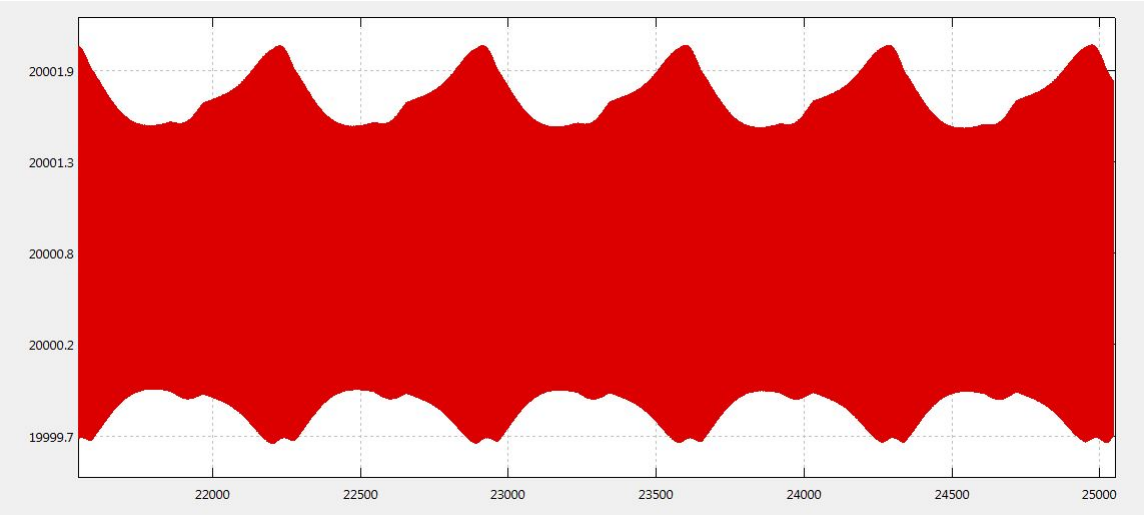

Figure 3.1: Trend of the SMA (y axis, expressed in km) in function of time (x axis, expressed in Modified Julian days).

x-axis points along the line formed by the intersection of the Mars mean equatorial plane and the mean ecliptic plane (at the J2000 epoch), in the direction of Aries. The z-axis is normal to the Mars mean equator at the J2000 epoch and the y-axis completes the right-handed system.

3.1.3 First test on the Gmat simulation

Before starting studying the viable orbits around Mars, it's better to make sure the simulation comprehends all the gravitational influences expected, like the one of the Sun. In Figure 3.1 is shown the trend of the SMA for a CubeSat in an aerostationary orbit. It's possible to see that there are some periodic maxima and minima in corrispondence of when Mars is at perihelion and their period is exactly the one of the revolution of Mars around the Sun (687 days).
In the mid way between two maxima, there's a little minimum: at first it was imputed to a orbital resonance with Earth, but this is not possible since Mars and Earth align about every 26 months (about 780) and this minimum should go nearer to its right maximum every Mars revolution completed. But this doesn't happen, so that must be imputed to another resonance due to the Sun.

3.2 Viable orbits around Mars

To find stable orbits around Mars is more complicated than on Earth due to two main factors:

- Mars has an anisotropic gravitational field.
  Thanks to the data from the Mars Orbiter Laser Altimeter (MOLA, an instrument of NASA's Mars Global Surveyor spacecraft) it was possible to create a digital elevation model of Mars. In this way a topographical atlas of Mars has been constructed, as shown in Figure 3.2. There's a difference in elevation between the hemispheres: the northern hemisphere is smooth, full of vallies while the southern hemisphere is heavily cratered, mountainous. The different density of the two hemispheres leads to an inhomogeneous gravitational field and that's why it is anisotropic.

- There are orbital resonances with the two natural Mars satellites: Phobos and Deimos.
  Orbital resonance happens when orbiting bodies perform regular, periodic gravitational influence on each other: usually tha main cause is that the orbital periods are related by a ratio of small intergers. Orbital resonances greatly enhance the mutual gravitational influence of the bodies. In most cases, this result in an unstable interaction: the bodies exchange momentum and shift orbits until the resonance disappears. For example, the orbital resonance between Deimos and Phobos (of which the ratio of number of orbits completed is $1:4$) causes a mismatch in orbital

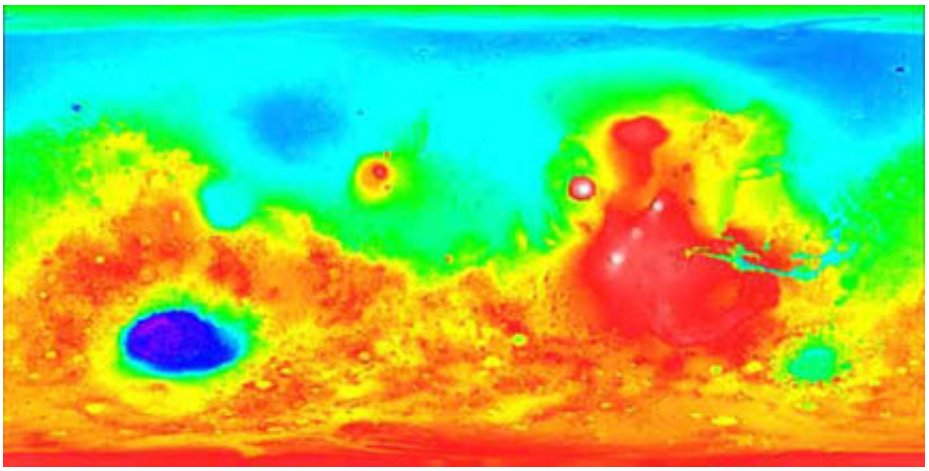

Figure 3.2: Flat map generated by the Mars Orbiter Laser Altimeter (MOLA), an instrument aboard NASA's Mars Global Surveyor, the high-resolution map represents 27 million elevation measurements gathered in 1998 and 1999. (Image credit: NASA)

longitude (i.e. the longitude of the ascending node) of Phobos compared to its position at the beginning of the cicle of 14.9 degrees, that is not negligible.

3.2.1 Low Mars Orbits

Low Mars Orbits are a good choice in term of cost of communications, as long as it takes less energy to send and receive informations from them. On the other hand, the dichotomy of Mars mass density and the consequential anisotropic gravitational field don't make this kind of orbits viable: indeed, chosen an equatorial, circular orbit with SMA= 550 km, the three CubeSats doesn't keep the mutual angular distance of 120 degrees and lose it after less then one year. It happens the same with orbits with SMA= 5000 km.
Adding the orbital resonance with Phobos, these kind of orbits are not viable at all. To have stable orbits for almost 4 years it's necessary to consider bigger SMAs.

3.2.2 Optimization of areostationary orbits for CubeSat Swarms

An areostationary orbit describes the motion of a satellite on the Mars equatorial plane and with the same period as the one of Mars rotation. It is one of the first chioices when thinking of orbits around the Red Planet, mostly because human settlments will be likely positioned on the equatorial area due to the warmer temperatures, but also because the communications with the satellites are easier in this way.
The ratio between Phobos period and the medium one of the three satellites in areostationary orbit is 1:3, and that means that the resonance can be a real problem (as said before).
CubeSats' orbital parameters chosen are shown in Table 3.1.

Table 3.1: Orbital parameters of the three CubeSats.

	CubeSat 1	CubeSat 2	CubeSat 3
SMA [km]	20002	20000	20000
ECC	0	0	0
INC [deg]	180	180	180
RAAN [deg]	0	0	0
AOP [deg]	0	0	0
TA [deg]	0	120	240

The value of the SMA is given by the radius expected for an areostationary orbit and it comes form

the third Kepler law:

$$r_{areos} = \sqrt[3]{\frac{GMT^2}{4\pi^2}} \tag{3.1}$$

In (3.1) G is the gravitational constant, M is the mass of Mars ($M = 6.4171 \cdot 10^{23}$ kg), T is the rotational period of Mars (88642 s). The result for the areostationary radius is:

$$r = 20428\,\text{km}$$

In Table 3.1, the SMA of CubeSat 1 is set at 20002 km while the one of CubeSat 2 and CubeSat 3 at 20000 km: this was necessary because during previous simulations it was seen that the orbit of CubeSat 1 with SMA equal to the one of CubeSat 2 and 3 was faster and due to this CubeSat 1 became really near to CubeSat 2 in a year, losing the equidistance of the three satellites.
The inclination is 180 degrees in order to make the orbit equatorial; the true anomaly, that defines the position of the orbiting body along the ellipse at a specific time, makes possible to put the three CubeSats at the mutual angular distance of 120 degrees, in order to guarantee that there's always a satellite between Mars and the Sun.
First of all, I monitored the trend of the satellites every three months of simulation for two years. The result was that the orbits were stable, and so the mutual angular distances between the CubeSats. Lately I simulated the orbits of the three CubeSats for 3500 days (about nine years) and I recorded the values of their orbital parameters for each year. The data collected are shown in Tables 3.2, 3.3, 3.4.

Table 3.2: Orbital parameters of the CubeSat 1.

	SMA [km]	ECC	INC [deg]	RAAN [deg]	AOP [deg]	TA [deg]
Year 0	20002.0	0.0	180.0	0.0	0.0	0.0
Year 1	20000.5	0.05	179.9	59.1	238.2	256.7
Year 2	19999.6	0.01	179.9	92.0	349.6	259.2
Year 3	20000.9	0.05	179.9	81.6	250.7	70.0
Year 4	20001.7	0.02	179.8	89.9	336.1	70.9
Year 5	20000.5	0.04	179.8	86.2	244.2	235.8
Year 6	19999.8	0.03	179.7	89.2	324.3	238.4
Year 7	20000.9	0.04	179.6	88.1	234.7	51.3
Year 8	20001.5	0.04	179.6	89.7	314.6	52.6
Year 9	20000.5	0.03	179.5	89.8	224.2	215.2

Table 3.3: Orbital parameters of the CubeSat 2.

	SMA [km]	ECC	INC [deg]	RAAN [deg]	AOP [deg]	TA [deg]
Year 0	20000.0	0.00	180.0	0.0	0.0	120.0
Year 1	19999.9	0.05	179.9	59.1	238.2	146.1
Year 2	20001.0	0.01	179.9	91.9	349.6	143.5
Year 3	20001.2	0.05	179.9	81.7	250.8	304.2
Year 4	20000.1	0.02	179.8	89.9	336.1	311.0
Year 5	19999.9	0.04	179.7	86.1	244.1	129.5
Year 6	20000.7	0.03	179.7	89.2	324.4	130.8
Year 7	20001.4	0.04	179.6	88.2	234.8	291.3
Year 8	20000.3	0.04	179.6	89.6	314.6	294.1
Year 9	19999.8	0.03	179.5	89.8	224.2	111.1

Table 3.4: Orbital parameters of the CubeSat 3.

	SMA [km]	ECC	INC [deg]	RAAN [deg]	AOP [deg]	TA [deg]
Year 0	20000.0	0.00	180.0	0.0	0.0	240.0
Year 1	20001.4	0.05	179.9	57.1	236.3	25.2
Year 2	20001.2	0.01	179.9	92.1	349.8	23.0
Year 3	19999.8	0.05	179.9	80.8	249.9	187.4
Year 4	19999.9	0.02	179.8	89.6	335.8	191.9
Year 5	20001.5	0.04	179.8	85.7	243.7	5.4
Year 6	20001.2	0.03	179.7	89.2	324.4	7.8
Year 7	19999.8	0.04	179.7	87.8	234.4	175.1
Year 8	19999.9	0.04	179.6	89.4	314.3	177.2
Year 9	20001.6	0.03	179.5	89.7	224.1	345.4

Comparing parameters INC and RAAN of the three CubeSats on each year, it's seen that they are similar, if not equal, that means the orbits stand still on the chosen equatorial plane. Also SMA and ECC are not affected by huge modifications, so the orbit keep being almost circular with an average SMA of 20000 km. In Table 3.5 are shown the differences between the TA of the three CubeSats (which we expect to be 120 degrees in order to have a full coverage from SEPs).

Table 3.5: Difference of the true anomalies of the three CubeSats in absolute value (C1 stands for CubeSat 1 and so on).

	TA(C2)-TA(C1) [deg]	TA(C2)-TA(C3) [deg]	TA(C3)-TA(C2) [deg]
Year 0	120.0	120.0	120.0
Year 1	110.6	120.9	128.5
Year 2	115.7	120.5	123.8
Year 3	125.8	116.8	117.4
Year 4	119.9	119.1	121.0
Year 5	106.3	124.1	129.6
Year 6	107.6	123.0	129.4
Year 7	120.0	116.2	123.8
Year 8	118.5	116.9	124.6
Year 9	104.1	125.7	130.2

Given a tolerance of 10 degrees, in the first four years the three CubeSats keep a satisfying equidistance, so they are able to detect any improvement of SEPs in order to give the alarm to human settlers.

Since this topic is the most important one, I collected all the TA's datas of the three CubeSats for all the duration of the simulation, then I computed the angular distance of each couple as a function of time. The result is shown in Figure 3.5. Angular distances should be ± 120 degrees or ± 240 degrees depending on the mutual position of the CubeSats.
In addition to the general trend, that in the first years is the one that we expected, there are some anomalies due to the orbital resonance with the Sun. Indeed, the strange variation of the difference of TAs happens when Mars is at perihelion, as in Figure 3.1 for the SMA. Nonetheless, this condition lasts few days and after those mutual angular distance become acceptable again.
With the passing of time, CubeSat 2 and 3 keep the equidistance, while CubeSat 1 and 3 tend to get closer: this is due to the effect of the anisotropic gravitational field, that giving a costant influence along time causes the crescent trend that can be seen in Figure 3.5 first and third.

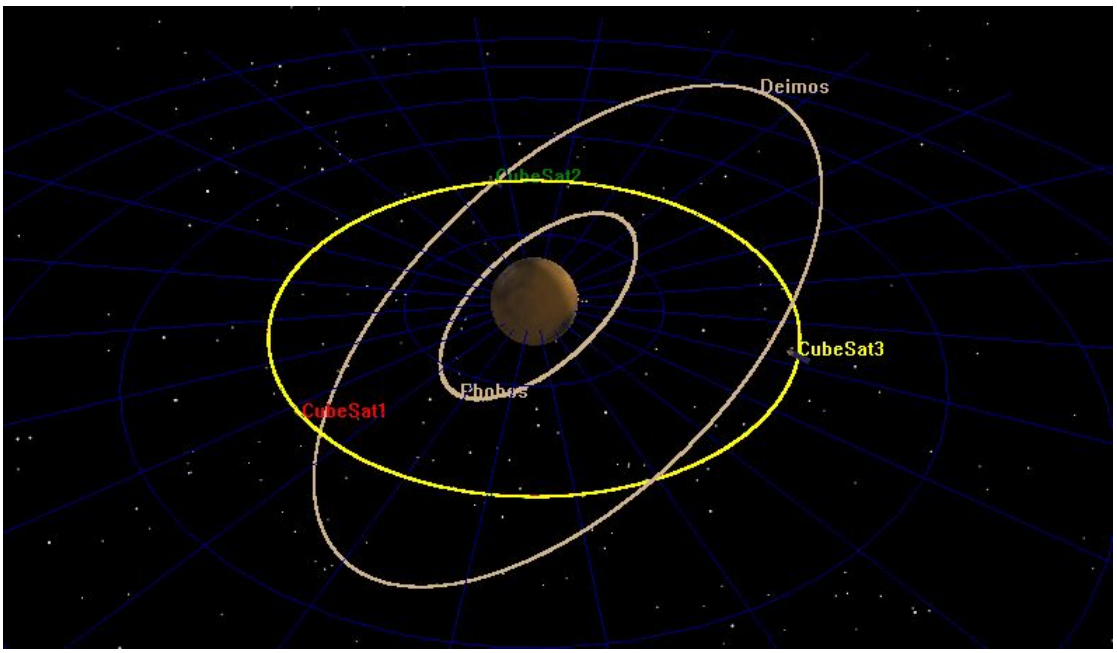

Figure 3.3: Disposition of the three CubeSats given by a simulation of two days starting from year 0 (CubeSat 1 is in red, CubeSat 2 is in green, CubeSat 3 is in yellow). The orbits in white are the one of Phobos and Deimos.

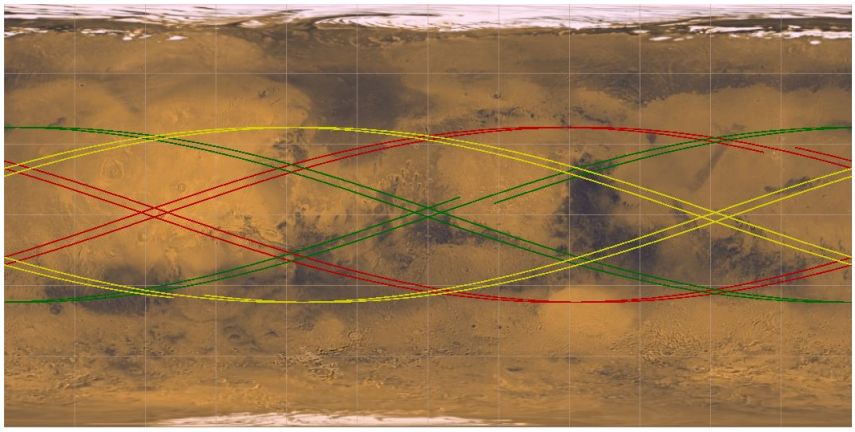

Figure 3.4: Ground track plot of the orbits of CubeSat 1 (in red), CubeSat 2 (in green) and CubeSat 3 (in yellow) given by a simulation of two days starting from year 0.

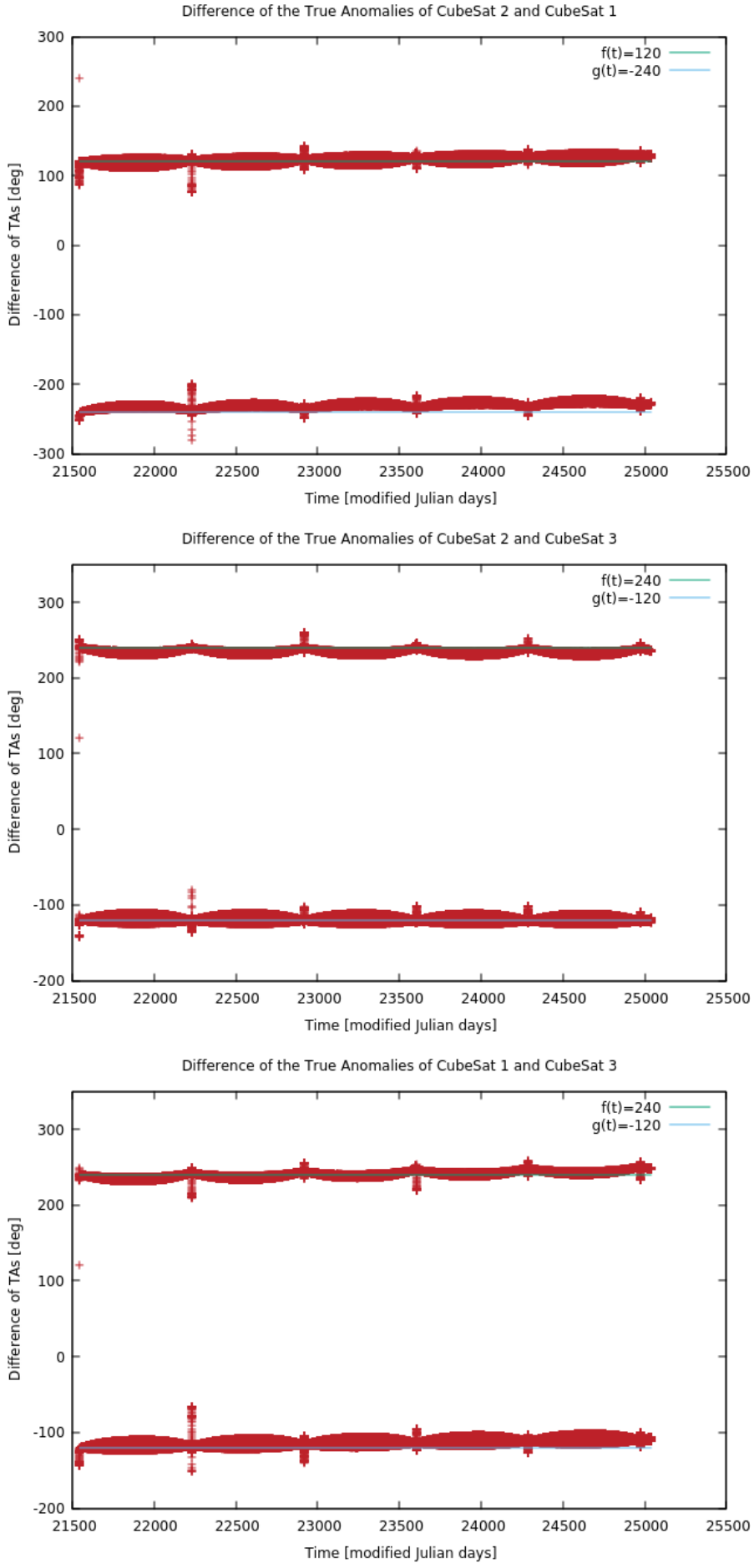

Figure 3.5: Difference of the TAs between each couple of CubeSats.

In Figure 3.4 we can see the ground track plot of the orbits of the three satellites: after one period, all three CubeSats do not come back to the initial positions, another effect caused by Mars gravitational influence.

A good Solar Radiation Alert System can be provided by CubeSats in the areostationary orbit described, and the protection from SEPs can be guaranteed for at least 5 years.

Conclusions

Solar radiation activity is potentially mortal for humans on Mars, hence the need for an effective alert system is urgent. In this work, we showed that a swarm of three CubeSats in areostationary orbit can provide a full coverage from SEP events for at least five years, giving the settlers an early warning to protect themselves.
Not only radiation poses a risk for astronauts while staying on the martian soil, dust storms may also prove fatal. In perspective, the three-satellite formation could be expanded at least to a tetrahedron, even if there will be difficulties due to the anisotropic gravitational field. The four CubeSats in this simple constellation could be equipped with large field of view visual cameras (tipically 60 degrees), in such a way that each satellite can monitor about π steradians of Mars surface, providing a full coverage and an early warning since the dust storms onsets.

Bibliography

[1] D.M. Hassler et al.: *Mars' Surface Radiation Environment Measured with Mars Science Laboratory's Curiosity Rover*, Science 343,6169 2014.

[2] G. Lucchetta et al.: *Scientific Performance of a Nano-satellite MeV Telescope*, The Astronomical Journal 153,237 2017.

[3] R. Rando et al.: *Sensitivity to gamma-ray bursts of a nano-satellite MeV Telescope with Silicon tracker*, The Astronomical Journal 158,1 2019.